

The Research of SURF Image Matching Method Based on Region and Feature Information

Rongbao Chen*, Qianlong Wang, Honghui Jiang, Yang Liu and Dawei Tang

Academy of electrical and automation engineering, Hefei University of Technology, Hefei 230009, Anhui Province China

*Corresponding author

Abstract—According to the SURF feature matching dense matching interpolation algorithm to realize the problems in the complex dynamic background image. The dynamic camera captured the same environment as the object. SURF image is proposed based on the combination of region and the feature information matching method. Firstly, image gray-scale normalization. There may be a reduction the brightness of light due to the translational response point of view. And then add several constraints in the process of extracting SURF feature points. Not only can speed up the matching process, but also can reduce the false match rate. Finally, in order to detect the feature points as the seed point for regional growth, the seed region division of the region by using graph matching. The test show that the algorithm can obtain dense disparity images of good. After the camera shooting of different sizes of image feature matching. Experiments show that, Compared with the SIFT algorithm and the SURF algorithm, the algorithm reduces the number of feature points and matching points, and improves the matching accuracy and the matching accuracy.

Keywords-SURF feature matching; dense matching; constraints; feature points; region matching

I. INTRODUCTION

In the image matching process, the main source of video images from the camera. If the camera is fixed, the video image obtained is the same. Used in road vehicle monitoring, only need to consider moving vehicle in the video image. If the camera is mounted on a mobile platform (such as an unmanned aerial vehicle), the image content of each adjacent video image is changed before and after each frame, which requires dynamic image matching. There are many mobile platforms that can mount the camera. It is very important to study the matching of dynamic camera images.

In 1999, D. G. Lowe proposed the famous SIFT algorithm. The SIFT algorithm mainly uses the pyramid Gaussian kernel filter model to decompose the image into several scale spaces, and extract the local characteristics of the extreme points in each layer. However, this method has the following problems: the number of successful matching points is small, the distribution is less uniform and the operation speed is slow and so on. In 2006, Herbert Bay et al. Proposed the SURF (Speed-Up Robust Features) algorithm, which is faster and more robust than the SIFT algorithm while maintaining the excellent characteristics of the SIFT algorithm. The difference between the two lies in the construction of multi-scale image space [1-4].

In the literature [2-3], the improved SURF algorithm can effectively remove the mismatch points, but the number of matching points is obviously less, and the matching images are relatively static images, which do not satisfy the dynamic image matching requirements. Although the advantage of SURF feature matching is that the matching speed is fast and the accuracy rate is relatively high. However, the feature matching between dynamic images needs to be a good interpolation algorithm to complete the dense matching, and the interpolation in complex dynamic background is often difficult to realize. The advantage of region matching is that a dense parallax image can be formed without interpolation. Because the gray information is susceptible to interference and similarity in the image, the ambiguity of matching cannot be solved perfectly. In order to achieve a higher quality match, this requires a large amount of computation or strong judgment conditions to guide the process of matching the region. Based on the above analysis, this paper first studies the principle of SURF algorithm, and puts forward the SURF image matching method based on the combination of region and feature information in the image taken by dynamic camera in the same environment.

II. FEATURE EXTRACTION AND DESCRIPTION OF SURF ALGORITHM

This article as a feature extraction algorithm of image matching algorithm using SURF The main process of SURF feature detection is divided into feature point extraction and feature SURF description vector. The flow chart of image feature matching is shown in figure 1.

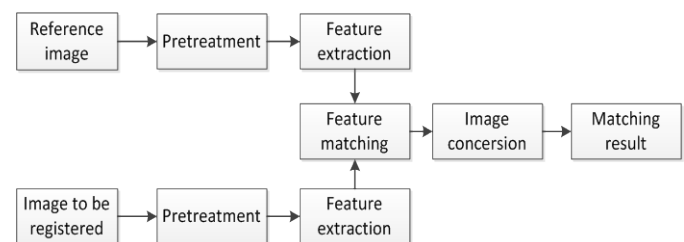


FIGURE 1. FLOW CHART OF FEATURE MATCHING

A. Feature Point Extraction of SURF Algorithm

The feature point detection of SURF algorithm is based on Hessian matrix [5]. For a pixel $s = (x, y)$ in image $I(x, y)$, the Hessian matrix $H(x, \sigma)$ is defined as:

$$H(x, \sigma) = \begin{bmatrix} L_{xx}(x, \sigma) & L_{xy}(x, \sigma) \\ L_{xy}(x, \sigma) & L_{yy}(x, \sigma) \end{bmatrix} \quad (1)$$

In the formula, $L_{xx}(x, \sigma)$ is the convolution of the two order derivative of the image $I(x, y)$ and Gauss function $G(x, y, \sigma)$ in the x direction in x. That is:

$$L_{xx}(x, \sigma) = I(x, y) * \frac{\partial^2}{\partial x^2} G(x, y, \sigma) \quad (2)$$

$$G(x, y, \sigma) = \frac{1}{2\pi\sigma^2} e^{-(x^2+y^2)/2\sigma^2} \quad (3)$$

$L_{xy}(x, \sigma)$ and $L_{yy}(x, \sigma)$ are similar with it. As shown in Figure 2 (a), suppose there is a template of size, followed by L_{xx} , L_{yy} , and L_{xy} from left to right.

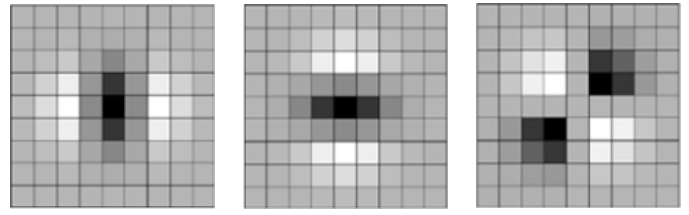
In order to improve the computation speed of Gauss convolution, the SURF operator uses box filter to approximate the two order Gauss filtering of $\sigma = 1.2$, and a Fast-Hessian matrix is constructed. The relationship between D_{xx} and D_{xy} and L_{xx} and L_{xy} is:

$$\omega = \frac{\|L_{xy}(1.2)\|_F \|D_{xx}(9)\|_F}{\|L_{xx}(1.2)\|_F \|D_{xy}(9)\|_F} \approx 0.9 \quad (4)$$

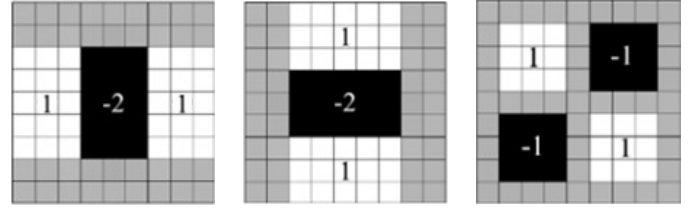
Formula: $\|\cdot\|_F$ is Frobenius norm, ω is weight coefficient, and 0.9 is used in actual application. Then the determinant of the Hessian matrix is:

$$\det(H_{essian}) = D_{xx}D_{yy} - (0.9D_{xy})^2 \quad (5)$$

The box filter template is shown in Figure 2 (b), and the black, gray, and white regions are weighted by -1, 0, and +1 respectively.



(a) Two order partial derivative template L_{xx} , L_{xy} and L_{yy}



(b) Box filter D_{xx} , D_{yy} and D_{xy}

FIGURE II. TEMPLATES AND WEIGHTED BOX FILTERS

Based on the Hessian matrix, the extremum of the scale image at (x, y, σ) is obtained. Firstly, non-maximum suppression is performed in the stereo neighborhood of the extremum point $3 \times 3 \times 3$ [6-7]. Only the extreme values which are larger or smaller than the 26 neighborhood values of the adjacent upper and lower scales and this scale can be used as candidate feature points. The location of the feature points and the scale values are obtained by interpolation.

B. Distribution of Feature Points and Determination of Main Directions

In order to make use of the integral graph to accelerate the operation, the SURF feature describes the Haar wavelet distribution of the statistical feature points in the X and Y directions instead of the gradient value distribution [8-10].

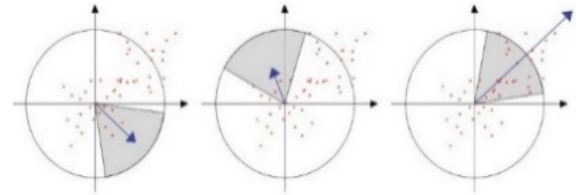


FIGURE III. FAN-SHAPED SLIDING WINDOW

As shown in Figure 3, the fan window with the center angle is slid with the characteristic point as the rotation origin. By accumulating the Haar wavelet response values in the sliding window, the amount of local information (m_w, θ_w) can be obtained.

$$\begin{cases} m_w = \sum_w d_x + \sum_w d_y \\ \theta_w = \arctan\left(\frac{\sum_w d_x}{\sum_w d_y}\right) \end{cases} \quad (6)$$

Since the Haar feature reflects the change in the image's gray level, the main direction is the direction of the region that describes the intensity of the gray change.

C. Generation of Feature Descriptors

After determining the principal direction of feature points, the local region near the feature points can be quantitatively described, and the descriptor [11-12], which is the descriptor of the feature points, is generated.

For the feature points, a central point is constructed along the main direction of the feature points. The size of the box near the center is $20s$ (s is the scale of the feature points). As shown in Figure 4, the sum of the wavelet responses is statistically calculated in the sub-region is $\sum d_x$ and $\sum d_y$, and the sum of its absolute values, and the four-dimensional descriptor vectors generated by $\sum |d_x|$ and $\sum |d_y|$.

$$V = (\sum d_x, \sum d_y, \sum |d_x|, \sum |d_y|) \quad (7)$$

Since the sub region of 4×4 is adopted, we can obtain a 64 dimensional feature vector of $4 \times (4 \times 4)$, which is a feature descriptor.

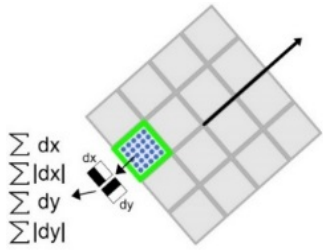


FIGURE IV. FEATURE DESCRIPTOR

III. SURF IMAGE MATCHING BASED ON REGION AND FEATURE INFORMATION

Firstly, several constraints are added to the extraction of SURF feature points, which can not only speed up the matching process, but also reduce the false matching rate of [13-14]. Before applying the SURF algorithm to the feature point matching, the gray level normalization is performed first, then the feature points are used as the seed points for the region growing, and the region matching of the seed regions is divided. This method not only combines the advantages of region matching without interpolation calculation, but also combines the effective information of feature points, which can effectively improve the matching accuracy and accuracy in the process of feature matching.

A. Matching Constraint

Finding matching pixels is essentially traversing the entire two-dimensional image. If an image contains n pixels, then the time complexity of this traversal is $O(n^2)$, which is clearly contrary to the real-time monitoring system indicators. Even the mismatch rate increases as the size of the image increases.

In order to reduce the computational complexity and improve the matching success rate, scholars have put forward some constraints:

(1) Disparity smoothness constraint. This requires a slow change in the parallax of most positions in the image. Assuming that the distance in the scene is not far from two points P and Q , the projection on the left and right images is P_l, P_r and Q_l, Q_r , then $\|P_l - P_r\| - \|Q_l - Q_r\|$ should be small.

(2) Ordinal constraint. As shown in Figure 5, consider the 3 feature points on the target surface, $A, B,$ and C , which are projected on two imaging images (along the pole line), exactly the reverse, for $C, B, A,$ and c', b', a' . The laws of the two opposite order are called ordinal constraints. This constraint helps to match the remaining points in the case where a partial match point pair has been determined on the pole line.

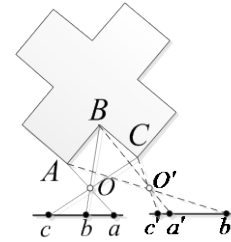


FIGURE V. SCHEMATIC DIAGRAM OF SEQUENTIAL CONSTRAINT

(3) Pole line constraint. Firstly, with the help of the binocular horizontal convergence mode as shown in Figure 6, there are two important concepts called pole C' and polar C'' in the heart of the left and right image plane, $C'C''$ is optical center line, which determines a plane called the "polar plane" with the object W . And the intersection of the left and right sides of the plane are called the left pole E' and the right pole E'' , the line L' and L'' of image plane and polar plane called polar according to the Figure 6.

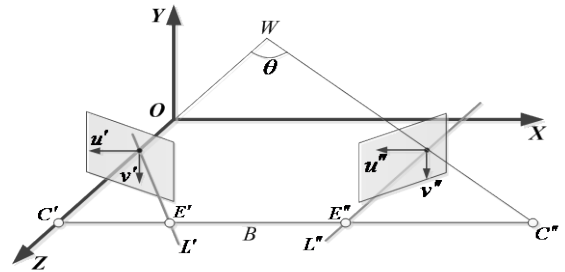


FIGURE VI. EPIPOLAR CONSTRAINT SCHEMATIC

"Pole line constraint" refers to the point W , respectively, in the left and right plane on the plane of the projection point must be on the same line. If a binocular parallel camera is used as the acquisition means of the image pair, the corresponding position of the corresponding feature point should ideally be satisfied at the same height under the condition of the line constraint. Considering that there is a change in grayscale in the actual

image capturing process due to image acquisition from different viewpoints, in the parallel view(the optical axes of the two cameras are parallel to each other), since the two pictures have no translation at the vertical height, there is only the horizontal direction of view to move. So that the constraint is changed correspondingly: If the corresponding matching point are two points on the image, $P_l(x_1, y_1)$ and $P_r(x_2, y_2)$, there is $y_1 = y_2$. Taking into account the shooting error and distortion factors, the search range for the matching pair is within the range of the upper and lower 7 columns. That is, if the corresponding matching point are two points on the image, $P_l(x_1, y_1)$ and $P_r(x_2, y_2)$, there is $|y_1 - y_2| \leq 3$.

For further consideration, set two pictures to be I_l and I_r , there must be a relationship between the feature points in the left image, $P_l(x_1, y_1)$ and the feature points in the corresponding right image, $P_r(x_2, y_2)$, that is $x_1 \geq x_2$. That position of the left feature points in the image feature point should be in the right position on the right image. In addition, according to the maximum parallax theory, the relative position difference of the corresponding matching point in the image is related to the vertical distance between the baseline length and the target distance camera, depending on the circumstances, the maximum parallax range may be refine search. We can improve the accuracy of matching, shorten the matching real-time, speed up the matching speed and reduce the wrong match rate under the effect of constraints.

B. Intensity Normalization

Before feathering point matching by using SURF algorithm, grayscale normalization preprocessing is performed [15-16]. Considering the reason for the point light of sight, there may be a luminance translation response. That is, the pixel gray value of a picture is higher than another one. So, it is necessary to do grayscale normalization preprocessing before extracting and matching feature points of an image. Normalization method: If the feature points on the left graph $P_l(x_1, y_1)$, so the location of the feature point P_r which is corresponding with P_l meets the condition: $\{P_r(x_2, y_2) | 0 \leq x_2 \leq x_1, |y_1 - y_2| \leq 2\}$. Therefore, the grayscale size of the point at coordinates (x, y) in the left image which is called $gray_L(x, y)$, then points of the right image in line with the above mentioned are called grayscale transformation.

$$gray'_R(x_i, y_j) = \frac{\max_L - \min_L}{\max_R - \min_R} \cdot (gray_R(x_i, y_j)) - \min_R \quad (8)$$

In the formula (8):

$$\begin{aligned} \max_R &= \max \{ gray_R(x_i, y_j) | 0 \leq x_i \leq x_r, |y_i - y_r| \leq 2 \} \\ \min_R &= \min \{ gray_R(x_i, y_j) | 0 \leq x_i \leq x_r, |y_j - y_r| \leq 2 \} \\ \max_L &= \max \{ gray_L(x_i, y_j) | 0 \leq x_i \leq x_l, y_i = y_l \} \\ \min_L &= \min \{ gray_L(x_i, y_j) | 0 \leq x_i \leq x_l, y_i = y_l \} \end{aligned} \quad (9)$$

$gray'_R(x_i, y_j)$ is the converted gray value, $gray_R(x_i, y_j)$ is the gray value before conversion. Then, SURF algorithm can be used to match the feature points of the image.

C. Regional Growth and Matching

By using the SURF matching method, the feature points in the image are initially detected and extracted, and then the localized regions are matched by the matching points. Schematic diagram of the growth of the seed area as shown in Figure 7, the region matching is sequentially performed from the pixel No. 0 in the order of the seed dots. In the process of matching, the sequential constraint is introduced at the same time, except for the constraint of the extreme line constraint and parallax smoothness constraint when the above feature points are used. For example, the 0th pixel in the figure is on the right side of the seed pixel (the feature point that has been successfully matched), so the corresponding matching point of the 0 pixel should be to the right of the corresponding point of the seed pixel. According to this constraint, the matching range can be greatly reduced, which can reduce the false matching rate, narrow the matching range, improve the matching efficiency, and realize the regional matching under the guidance of the feature points.

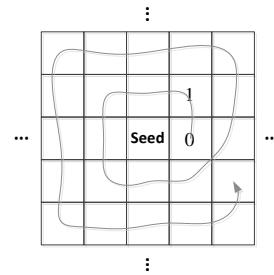


FIGURE VII. REGIONAL GROWTH DIAGRAM

Defining the following two constraints to ensure that the region under growth is still under the constraint of the seed.

① In the formula (10), when the numbers rows and columns of growth area of the pixels $P_G(i, j)$ and the absolute value of seed points $P_s(x, y)$ are more than 15, the region growth process is ended.

$$(|i-1| + |j-y|) \leq 15 \quad (10)$$

② In the area grows, when the growth point enters the area of the other seed(The range of the region is generated and marked by the SURF characteristics growth, feature points

around the pixel area are 8×8), the seed growth is stopped and transferred to the next seed growth process.

In order to ensure the matching accuracy, the threshold Y is defined. When the matching degree is less than Y in the process of regional growth matching, the regional growth matching process of the seed will be stopped. It can achieve accurate and rapid regional matching according to these two constraints. The process of the algorithm is shown in Figure 8.

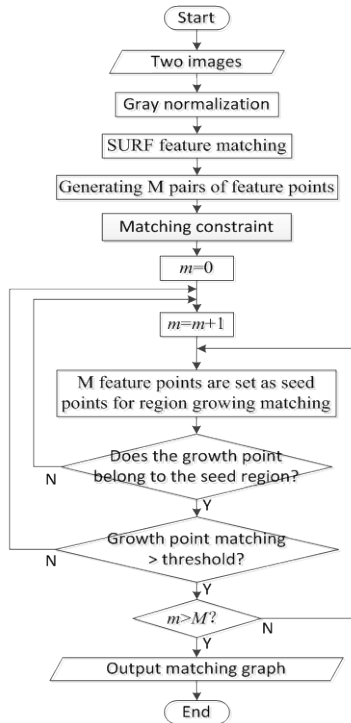
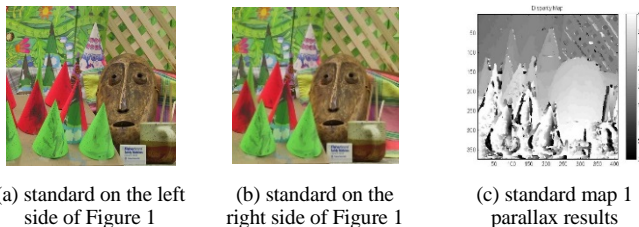


FIGURE VIII. IMPROVED MATCHING ALGORITHM FLOW

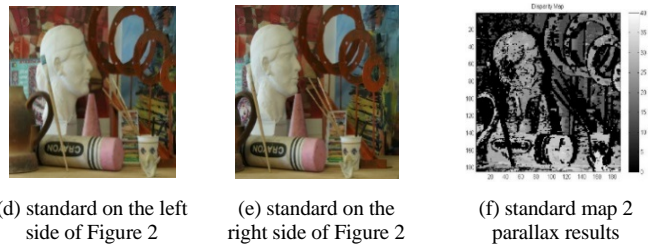
IV. EXPERIMENTAL RESULTS AND ANALYSIS

In this paper, the author selected the standard used in image matching field, used the graph to test the performance of the improved algorithm, and then matched the actual scene pictures taken from the camera.

As shown in Figure 9, the left and right graphs of the two standard pictures are respectively matched to obtain a parallax image.



(a) standard on the left side of Figure 1 (b) standard on the right side of Figure 1 (c) standard map 1 parallax results



(d) standard on the left side of Figure 2 (e) standard on the right side of Figure 2 (f) standard map 2 parallax results

FIGURE IX. IMAGE MATCHING CRITERIA USING GRAPHS PARALLAX RESULTS

As shown in Table 1, the matching key points (seed points) of the two pictures are presented

TABLE I. MATCHING OF KEY POINTS IN STANDARD DRAWING

	Figure 1	Figure 2
The key points of the left figure	1042	493
The key points of the right figure	1086	488
Characteristic point repetition rate	95.90%	99.00%

As shown in Table 1, since some areas do not have obvious textural features, there are no matching points after the region grows, so the repetition rate of feature points is not 100%; In addition, because of the mutual occlusion of objects between left and right, there is no critical point in these blocks, and then the region cannot grow. These reasons are reflected in the disparity map, which is represented by the emergence of an empty region. Nevertheless, parallax results can still be obtained with relatively complete depth information as shown in Fig. 9 (c) and 9 (f).

By using the SURF image matching method which combines the region and feature information, this paper did the matching experiments on the standard images used in image matching field. The experiment selected two images in the same environment for verification, as shown in Figure 10 (a) and figure 10 (b).



FIGURE X. ACTUAL CAPTURED IMAGES

After the gray level transformation, the feature points are detected by the SURF algorithm, as shown in figure 11.

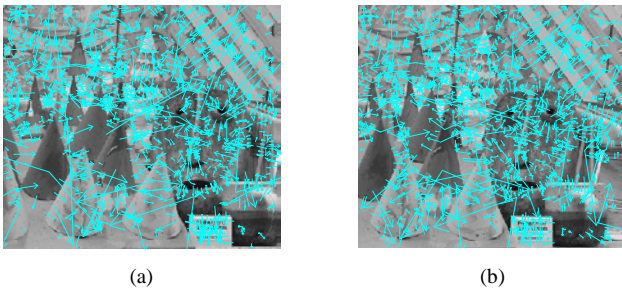


FIGURE XI. GRAPHS OF FEATURE POINTS DETECTED BY SURF ALGORITHM

The feature point matching wiring diagram is shown in figure 12.

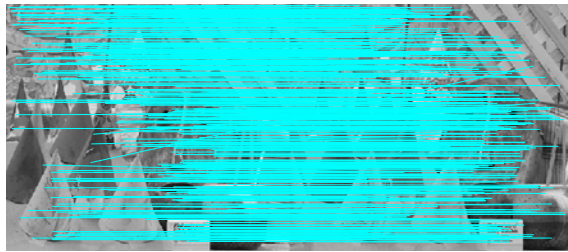


FIGURE XII. SCHEMATIC DIAGRAM OF MATCHING LINE BY FEATURE POINTS OF SURF ALGORITHM

In Figure 12, you can see a total of 414 pairs of matching feature point pairs, 18 pairs of false feature points, which shows that the rate of false registration is higher, and the matching effect is not ideal. After matching the region and feature information, the SURF image matching method is used to match the feature points after image processing, as shown in figure 13.

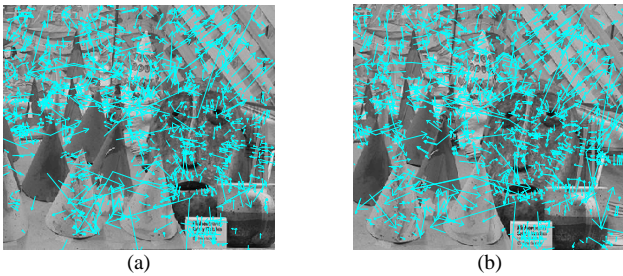


FIGURE XIII. GRAPHS FOR DETECTING FEATURE POINTS USING THE PROPOSES ALGORITHM IN THIS PAPER

The feature point matching wiring diagram is shown in figure 14.

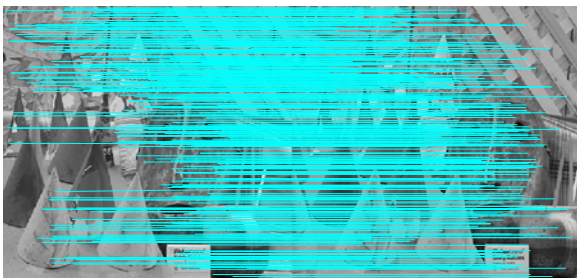


FIGURE XIV. SCHEMATIC DIAGRAM OF MATCHING LINE USING FEATURE POINTS OF THE ALGORITHM IN THIS PAPER

TABLE II. THE SURF ALGORITHM MATCHES THE RESULTS OF THIS ALGORITHM

	SURF algorithm	Paper algorithm
Characteristic points of figure a	1042	862
Characteristic points of figure b	1086	874
Logarithmic characteristic points of matching	414	387
Logarithmic characteristic points of incorrect matching	18	2

From table 2 and Figure 15, you can see that compared with SURF algorithm, the use of the improved SURF algorithm to detect the original text, the feature points of matching graphs and the matching feature points have all decreased, but the number of mismatching points is obviously lower, and the matching effect is better.

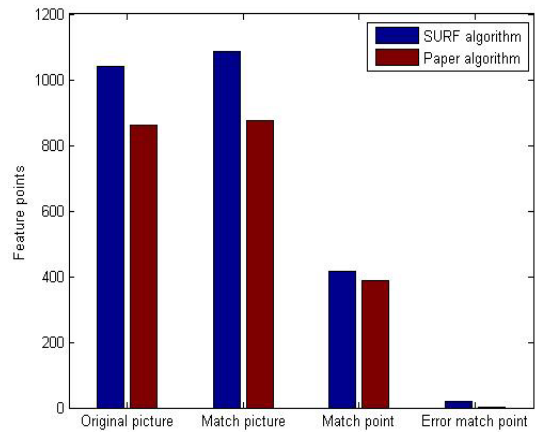
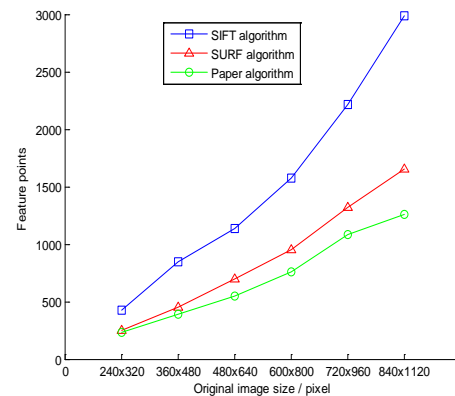


FIGURE XV. THE MATCHING RESULTS OF SURF ALGORITHM AND THE ALGORITHM IN THIS PAPER

In order to further illustrate the advantages of this algorithm, this paper performed multiple sets of images of different sizes and compared the results, the results are shown in figure 16.



(a) Comparison of the number of feature points of original image

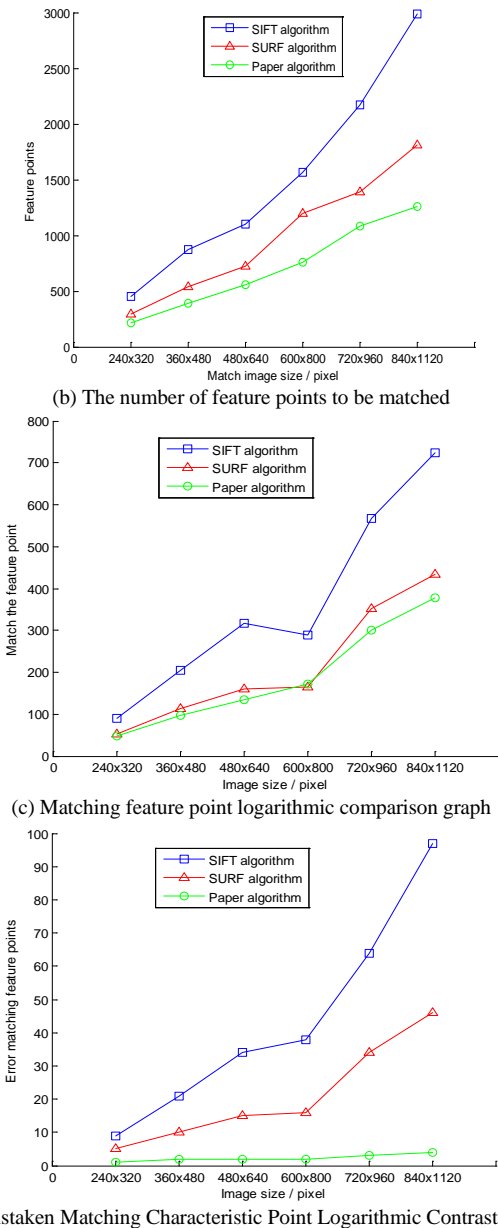


FIGURE XVI. DIFFERENT IMAGE SIZE MATCHING RESULTS CONTRAST GRAPHS OF SIFT ALGORITHM, SURF ALGORITHM, AND THIS ALGORITHM IN THIS PAPER

From Figure 16, you can see that compared with the SIFT algorithm, SURF algorithm, this algorithm added matching constraints, and the characteristic of region growing to achieve local matching, so that the number of characteristic points are reduced, the number of matched points are reduced, and some pseudo matching is removed. However the matching accuracy and the matching accuracy have been greatly improved

V. CONCLUSION

In this paper, the author studied a SURF matching algorithm based on region and feature information, and solved the problem that SURF feature matching algorithm is difficult to implement in dense and dynamic context. First of all, the image is normalized by gray level, so as to reduce the

brightness shift response due to the influence of light viewpoint. Then, the matching constraints are used to detect the feature points, so as to speed up the matching process and reduce the false matching. Moreover, the detected feature points are used as seed points for regional growth, and the region matching of the seed regions is carried out to improve the density matching accuracy and the matching accuracy. The author conducts experiments on standard map and images of different sizes, which proves that compared with SIFT algorithm and SURF algorithm, the algorithm in this paper reduced the feature point detection and matching point pairs, the matching accuracy and matching accuracy has a significant advantage, finally realized the corresponding image for dense dynamic image matching on the field of mobile platform. It has important practical significance for road vehicle dynamic video surveillance and aerial unmanned aerial vehicle tracking.

REFERENCES

- [1] Peng Hui, Wen Youxian, Zhai Ruifang, et al. Combining SURF operator and polar line constrained citrus stereo image pair matching [J]. Computer Engineering and Applications, 2011, 47 (8): 157-160.
- [2] WEI Xin, MA Li-hua, LI Yun-xia, et al. Fast registration algorithm for SUFT infrared image based on improved registration measure [J]. Electro-Optic and Control, 2012, 19 (11): 77-80.
- [3] ZHAO Lulu, GENG Guohua, LI Kang, et al. Image Matching Algorithm Based on SURF and Fast Approximation Nearest Neighbor Search [J]. Application Research of Computers, 2013, 30 (3): 921-923.
- [4] WANG Shuiyuan, MA Yu, WANG Yuanyuan. Medical CT Image Retrieval Based on SIFT Feature and Approximate Nearest Neighbor Algorithm [J]. Advances in Biomedical Engineering, 2011, 32 (3): 123-129.
- [5] Jiang P, Zhao S, Cheng S. Rotational invariant LBP-SURF for fast and robust image matching[C]// International Conference on Signal Processing and Communication Systems. IEEE, 2015:1-7.
- [6] Sergieh H M, Egyedzsigmond E, Doller M, et al. Improving SURF Image Matching Using Supervised Learning[C]// Eighth International Conference on Signal Image Technology and Internet Based Systems. IEEE, 2012:230-237.
- [7] Saygili G, Maaten L V D, Hendriks E A. Improving segment based stereo matching using SURF key points[C]// IEEE International Conference on Image Processing. IEEE, 2013:2973-2976.
- [8] Jia X, Wang X, Dong Z. Image matching method based on improved SURF algorithm[C]// IEEE International Conference on Computer and Communications. IEEE, 2016:142-145.
- [9] Ma Y L S. Research on Image Based on Improved SURF Feature Matching[C]// Seventh International Symposium on Computational Intelligence and Design. IEEE, 2015:581-584.
- [10] Szczuko P. Influence of image transformations and quality degradations on SURF detector efficiency[J]. 2013:285-290.
- [11] Zhang X, Hirai S. TPS-SURF-SAC matching approach of feature point applied to deformation measurement of nonrigid tissues from MR images[C]// IEEE International Conference on Robotics and Biomimetics. IEEE, 2011:551-556.
- [12] Jing L, Xu L, Li X, et al. Determination of platform attitude through SURF based aerial image matching[C]// IEEE International Conference on Imaging Systems and Techniques. IEEE, 2014:15-18.
- [13] Du M, Wang J, Li J, et al. Robot robust object recognition based on fast SURF feature matching[C]// Chinese Automation Congress. IEEE, 2013:581-586.
- [14] Suaib N M, Marhaban M H, Saripan M I, et al. Performance evaluation of feature detection and feature matching for stereo visual odometry using SIFT and SURF[C]// Region 10 Symposium. IEEE, 2014:200-203.
- [15] Nemra A, Slimani S, Bouhamidi M, et al. Adaptive Iterative Closest SURF for visual scan matching, application to Visual odometry[C]// International Conference on Systems and Control. IEEE, 2014:927-932.

- [16] Tao L, Jing X, Sun S, et al. Combining SURF with MSER for image matching[C]// IEEE International Conference on Granular Computing. IEEE, 2013:286-290.